Ultra-Local Model Based Sensorless Predictive Control for Induction Motor Drives

Lu Zhang[1], Yanghai Wang[1], Ziwei Dong[1*], Yingqian Zhang[1], Jiayue Hou[1]
[1]Department of Electrical Engineering, Beijing Institute of Petrochemical Technology, 102617, Beijing, China
Corresponding author: Ziwei Dong (email: dongziweibipt@163.com)

ABSTRACT Sensorless model predictive control (MPC) of induction motors is highly sensitive to parameter uncertainties and speed estimation errors, which may degrade system performance and stability. To overcome these limitations, an ultra-local model based sensorless predictive control strategy is developed in this study. The induction motor is first modeled in the stationary two-axis reference frame, and the implementation process of the predictive control algorithm is described. To eliminate the need for a mechanical speed sensor, a full-order adaptive observer is designed to reconstruct rotor speed and flux linkage information in real time. Considering the influence of parameter variations, external disturbances, and modeling inaccuracies during operation, an ultra-local dynamic representation is introduced to capture the system behavior without relying heavily on precise motor parameters. Furthermore, a sliding mode observer is employed to estimate and compensate for lumped disturbances, thereby improving the disturbance rejection capability and robustness of the control system. The proposed approach is validated through Matlab/Simulink simulations under different operating scenarios, including parameter perturbations, speed changes, and load disturbances. The simulation results indicate that the proposed method can accurately reconstruct rotor speed while preserving desirable dynamic and steady-state characteristics. Compared with conventional sensorless MPC schemes, the proposed control strategy demonstrates enhanced tolerance to parameter mismatches and stronger resistance to external disturbances. These findings confirm the effectiveness of the proposed approach and its potential application in high-performance sensorless induction motor drive systems.

INDEX TERMS Induction motor; Model predictive control; Ultra-local model; Adaptive full-order observer; Sensorless control

I. INTRODUCTION

WITH the continuous advancement of global energy conservation and low-carbon development, high-efficiency motor drive systems have become an important research topic in modern industry. induction motors are widely employed in factories, transportation vehicles, electric vehicles (EVs), and industrial automation due to their simple structure, low cost, high reliability, and strong environmental adaptability[1]. However, induction motors are characterized by strong nonlinearity and coupling, and their performance is easily affected by parameter variations and load disturbances, which makes high-performance control a challenging task[2].

As of now, the major control method for Induction Motors has been V/F (Variable Voltage & Frequency Control), DTC (Direct Torque Control), FOC (Field-Oriented Control), MPC (Model Predictive Control) etc[3]. V/F features a simple structure and low implementation cost, but its dynamic response performance is relatively poor. DTC provides fast torque response; however, it usually suffers from large torque and current ripples[4]. FOC can realize decoupled control of flux and torque and has been widely applied in industrial systems, but its control performance strongly depends on accurate motor parameters and coordinate transformation precision[5].

Traditional motor drive systems usually employ mechanical sensors such as encoders or tachogenerators to obtain speed information[6]. However, these sensors increase system cost, installation complexity, and maintenance difficulty, while their reliability may decrease under harsh operating conditions such as high temperature, humidity, and vibration. Therefore, sensorless control has gradually become an important research direction in induction motor drive systems. Existing sensorless methods mainly include model reference adaptive systems, sliding-mode observers, Kalman filters, and adaptive full-order observers[7]. Among them, adaptive full-order observers can simultaneously estimate rotor speed and flux linkage, making them suitable for MPC-

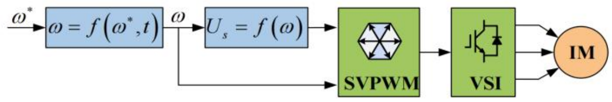

FIGURE 1. Structure of the induction motor V/f control scheme

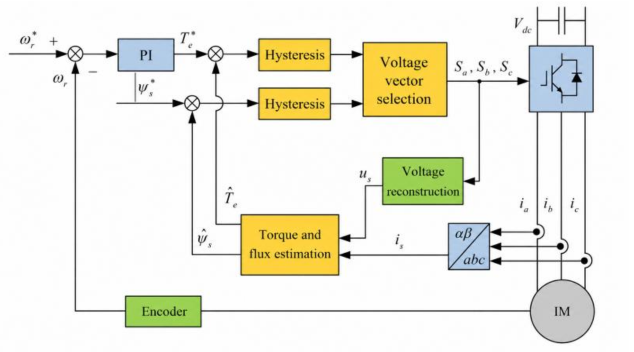

FIGURE 2. The Diagram of Induction Motor Direct Torque Control

based drive systems.

II. LITERATURE REVIEW

Variable Voltage and Variable Frequency(V/F) control is to keep a fixed ratio of output voltage to supply frequency so that we have roughly same flux in our motors. So it's also known as Constant Flux Control. And you don't need the type of the feedback signal like velocity and current etc. Then you might say that is kind of an open loop system controlling your speed. The block diagram of the control algorithm is shown in Fig. 1. The good sides of V/F control are easy structure, low price, good enough for things needing not much dynamic behavior. However, when the frequency decreases while the voltage remains constant, magnetic saturation may occur, which can even damage the motor[8]. In addition, the system may suffer from oscillation and poor dynamic response, especially in high-power systems with small inertia. To improve low-speed performance and operating efficiency, previous studies proposed stator resistance compensation and closed-loop V/F control strategies using PI controllers[9].

Direct torque control(DTC) uses electromagnetic torque and stator flux linkage as controlled variables. Torque and flux error are processed by using hysteresis comparator to get the optimum voltage vector from switching table for controlling the Inverter[10]. Induction motor direct torque control diagram is shown in Figure 2. Compared with conventional vector control, DTC eliminates the modulation stage and provides fast dynamic response for torque and flux control. However, the switching frequency is not fixed, and only eight basic voltage vectors are available, which results in large torque and current ripple[11].

III. INDUCTION MOTOR MODEL PREDICTIVE CONTROL FRAMEWORK

A. MATHEMATICAL DESCRIPTION OF THE INDUCTION MOTOR

An induction motor is a nonlinear strongly coupled and multi-variable system as seen below in Figure 3. Control design has been made simpler by the mathematical model which is generally transformed into a two-phase stationary coordinate from a three phase stationary coordinate system.

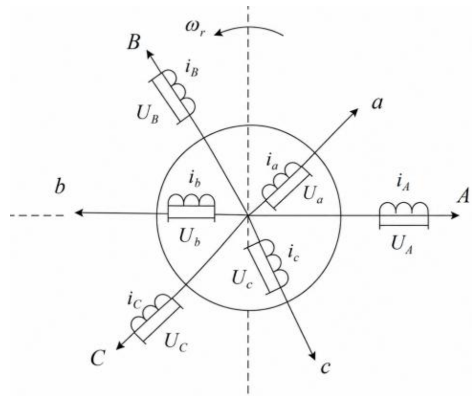

FIGURE 3. Schematic representation of the induction motor

B. BASIC PRINCIPLE OF MPC

Using finite control set model predictive control to predict the future states of the controlled variable based on the motor model. Assuming the switching action is A_i, we have the estimated value for the controlled variable, which is[13]:

$$x_{k+1} = f_p(x_k, A_i), \quad i = 1, 2, \dots, n \tag{1}$$

The cost function is constructed as:

$$g_i = f_g(x^*, x_{k+1}), \quad i = 1, 2, \dots, n \tag{2}$$

To minimize the tracking error, it can be written as:

$$g_i = |x^* - x_{k+1}|, \quad i = 1, 2, \dots, n \tag{3}$$

When another control variable $y(t)$ is included, the cost function becomes:

$$g_i = |x^* - x_{k+1}| + \gamma |y^* - y_{k+1}|, \quad i = 1, 2, \dots, n \tag{4}$$

IV. SENSORLESS PREDICTIVE CONTROL USING A FULL-ORDER ADAPTIVE OBSERVER

In conventional induction motor drive systems, rotor speed is generally obtained using mechanical sensors such as encoders. However, speed sensors increase system cost and reduce reliability under harsh operating conditions. Therefore, sensorless control technology has become an important research topic in induction motor drive systems. In this chapter, a full-order adaptive observer is incorporated into the MPTC system to achieve online estimation of rotor speed and flux linkage.

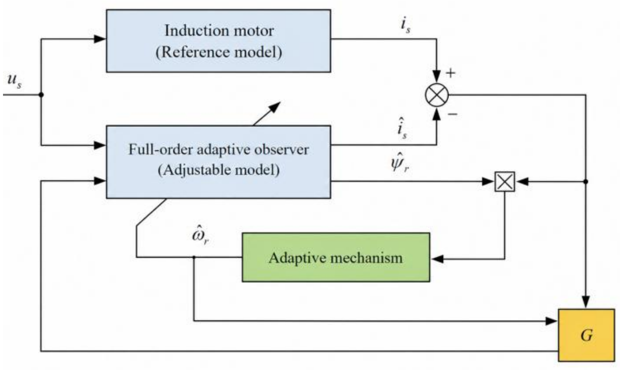

FIGURE 4. Configuration of the proposed full-order adaptive observer

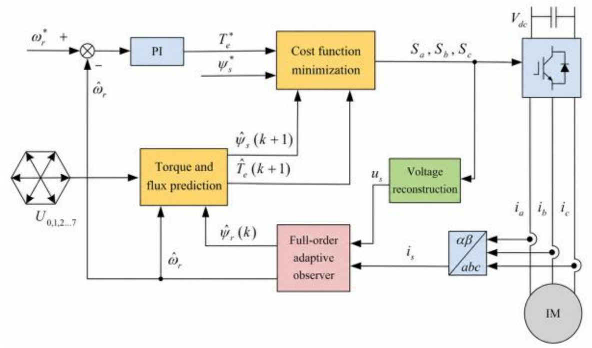

FIGURE 5. Sensorless MPTC Based on Full-Order Adaptive Observer

According to Induction Motor Mathematical Model on Fixed System Coordinate System, it is the equation which expresses[14]:

$$\begin{cases} \dot{x} = Ax + Bu \\ y = Cx \end{cases} \tag{5}$$

Full-Order Adaptive Observer equation[15]:

$$\begin{cases} \dot{\hat{x}} = A\hat{x} + Bu + G(i_s - \hat{i}_s) \\ \hat{y} = C\hat{x} \end{cases} \tag{6}$$

where the estimated state vector, and represents the structure of the full-order adaptive observer is shown in Fig. 4.

To improve the estimation accuracy, the observer poles are designed using the pole assignment method. Meanwhile, the rotor speed adaptive law is established according to Lyapunov stability theory as[16]:

$$\hat{\omega}_r = \left(k_p + \frac{k_i}{s}\right)\left(e_{is\alpha}\hat{\psi}_{r\beta} - e_{is\beta}\hat{\psi}_{r\alpha}\right) \tag{7}$$

where Kp and Ki are proportional coefficient and integrative one respectively.

We pick Lyapunov function to be:

$$V = e^T Pe + \frac{1}{\gamma}(\omega_r - \hat{\omega}_r)^2 \tag{8}$$

When the observer system is asymptotically stable.

$$\dot{V} < 0 \tag{9}$$

The voltage vector corresponds to the minimum cost function value, which we select then apply it to the inverter. Overall structure of the sensorless predictive control system as shown in Fig. 5. Compared with the traditional MPTC plan, the plan we are discussing here does not use a mechanical speed sensor and will make the system better. Full-Order Adaptive Observer estimates well Rotor Speed and Rotor Flux Linkage making the Induction Motor System more responsive (Dynamic) as well as stable (Static). But it should be noted that this prediction model still relies on these motor parameters, so if there is any problem like different motor parameters fitting or observation error, etc., it will affect the robustness of the predict control system[17].

V. SENSORLESS PREDICTIVE CONTROL USING AN ULTRA-LOCAL DYNAMIC MODEL

A. RATIONALE FOR INTRODUCING THE ULTRA-LOCAL MODEL

In the common model predictive torque control without sensors, the prediction accuracy relies heavily on the motor's specifications and guessed rotating pace details. During long- term operation, motor parameters may vary because of temperature rise, magnetic saturation, and load disturbance. In addition, the full-order adaptive observer may also introduce speed estimation error. These factors directly affect the prediction of stator current, torque, and flux, and finally lead to a non-optimal voltage vector selection in the cost function. Therefore, the robustness of the conventional sensorless MPTC system is limited under parameter mismatch conditions[18].

In the original thesis, parameter sensitivity is first analyzed from two aspects: the model predictive control algorithm and the full-order adaptive observer. The results show that when the stator resistance or mutual inductance is mismatched, the estimated flux amplitude and phase both deviate from the actual values. In particular, stator resistance mismatch has a more obvious influence at low speed. Mutual inductance mismatch also affects the flux amplitude and phase. It becomes particularly true as the system begins operating at very slow velocities. These errors will be propagated throughout the prediction process, leading to inaccurate stator-current prediction and further deteriorating the electromagnetic torque[19].

These results (Figs. 6-9) lead me to think it is sensitive to motor parameters. Prediction models using incorrect rotorspeed or flux data will not find the right choice during the rolling opti mization process when they have it wrong about those things. Problem: So instead we use an ultralocal model for the parameter depending predicting model.

B. FUNDAMENTAL PRINCIPLES OF THE ULTRA-LOCAL MODEL

Ultra-local comes from Michel Fliess's work on model free control. Its main idea is that the system can be described only by input and output data, without relying on an accurate mathematical model of the controlled object. Therefore, it has strong robustness against internal disturbance, external disturbance, and unmodeled dynamics[20].

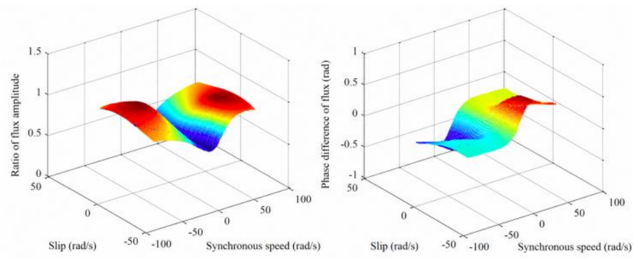

FIGURE 6. Waveform Between Synchronous Speed, Slip and Flux Amplitude and Phase Difference, 1.5Rs

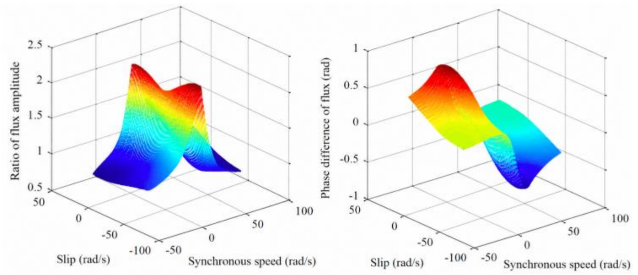

FIGURE 7. Waveform Between Synchronous Speed, Slip and Flux Amplitude and Phase Difference, 0.5Rs

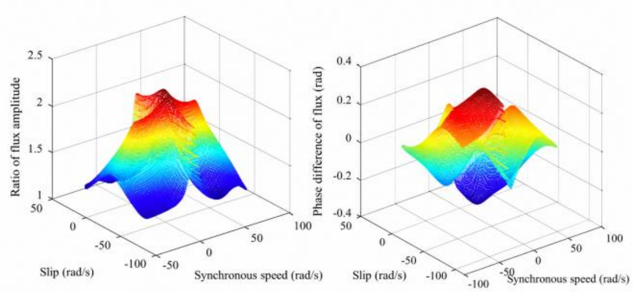

FIGURE 8. Waveform Between Synchronous Speed, Slip and Flux Amplitude and Phase Difference, 1.5Lm

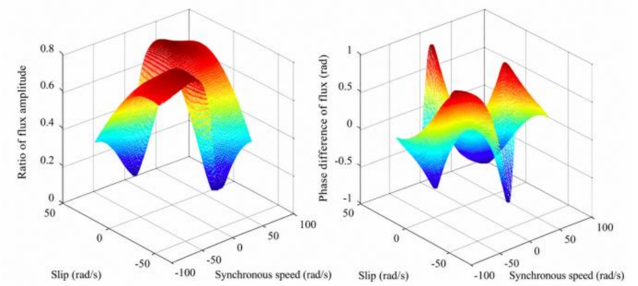

FIGURE 9. Waveform Between Synchronous Speed, Slip and Flux Amplitude and Phase Difference, 0.5Lm

For a SISO (Single Input Single Output), it can be expressed as:

$$E(y, \dot{y}, \ldots, y^{(a)}, u, \dot{u}, \ldots, u^{(b)}) = 0 \tag{10}$$

According to the model-free control theory, equation can be rewritten as the following ultra-local model:

$$y^{(v)} = F + \alpha u \tag{11}$$

Where v is the order of the system; α is the coefficient of the input variable, F represents the unknown portion that is based upon the inputs to the system and its outputs. The term F has internal dynamics, external disturbance, parametric mismatch and modeling uncertainty of the system. Compared with the common induction motor math model, ultra-local model doesn't need those parameter like stator resistance, rotor resistance, leakage inductance, mutual inductance and rotor speed. So we can use this model to improve the robustness of the sensorless model prediction control.

C. PREDICTIVE CONTROL DESIGN BASED ON ULTRA-LOCAL MODELING

According to the original thesis, the conventional prediction model uses the estimated rotor speed obtained from the full-order adaptive observer. When the estimated speed has a large error, the predicted stator current also becomes inaccurate. This may lead to an incorrect switching vector selection and degrade both dynamic and steady-state performance. Meanwhile, the estimation error is also fed back to the observer, further affecting the speed estimation accuracy. To overcome this problem, the prediction model is redesigned by introducing the ultra-local model.

Based on the induction motor model under the two-phase stationary coordinate system, the ultra-local model expressions for the α-axis stator current, and the β-axis stator current, respectively are as follows:

$$\begin{cases} \dfrac{di_\alpha}{dt} = F_\alpha + a_\alpha u_\alpha \\ \dfrac{dF_\alpha}{dt} = f_\alpha \end{cases} \tag{12}$$

$$\begin{cases} \dfrac{di_\beta}{dt} = F_\beta + a_\beta u_\beta \\ \dfrac{dF_\beta}{dt} = f_\beta \end{cases} \tag{13}$$

Through this formulation, the stator current prediction no longer depends directly on the original complex motor parameter model. The unknown term F absorbs the effects of parameter mismatch, load disturbance, and speed estimation error. Therefore, the predicted stator current can be corrected online, which helps maintain the optimality of the selected voltage vector.

D. DESIGN OF THE ULTRA-LOCAL SLIDING MODE OBSERVER

Although the ultra-local model reduces parameter dependence, the unknown term F still needs to be estimated accurately. In the original thesis, it is pointed out that when F changes suddenly, such as under load mutation or parameter mutation, differential algebraic estimation might be very sluggish due to using a great deal of historical data. Dynamic response is improved with a ultra-local sliding mode observer.

According to the induction motor ultra-local model, the sliding mode observer for the α-axis is made like so:

$$\begin{cases} \dfrac{d\hat{i}_\alpha}{dt} = \hat{F}_\alpha + a_\alpha u_\alpha + U_{\alpha smo} \\ \dfrac{dF_\alpha}{dt} = g_\alpha U_{\alpha smo} \end{cases} \tag{14}$$

The sliding mode observer for the β-axis is

$$\begin{cases} \dfrac{d\hat{i}_\beta}{dt} = \hat{F}\beta + a\beta\, u\beta + U_{\beta smo} \\ \dfrac{dF_\beta}{dt} = g\beta U_{\beta smo} \end{cases} \tag{15}$$

where F_α and F_β are the estimated values of F_α and F_β, respectively. i_α and i_β are the estimate of stator current in the α axis. And also $U_{\alpha smo}$, $U_{\beta smo}$ is the sliding control function, g_α, g_β is the sliding parameter.The stability of the sliding mode observer is analyzed using the Lyapunov method. According to the original derivation, combining equations the following relationship is obtained for the α-axis:

$$\dot{V}_\alpha = e_1 e_2 - k|e_1| - \lambda e_1^2 \tag{16}$$

To satisfy the stability condition, the sliding mode parameter should meet $k_1 > |e_2|$.

$$\begin{aligned} \dot{V}_\beta &= e_3\dot{e}_3 = e_3(e_4 + U_{\alpha smo}) \\ &= e_3[e_4 - k\,\mathrm{sgn}(e_3) - \lambda e_3] \\ &= -[-e_3e_4 + e_3(k\,\mathrm{sgn}(e_3)) + \lambda e_3^2] \end{aligned} \tag{17}$$

Thus, the sliding mode parameter should also satisfy $k > |e_4|$. In summary, the sliding mode parameter is selected according to:

$$k > \max(|e_2|, |e_4|) \tag{18}$$

These equations are the final discrete forms used in the ultra-local model-based prediction process. By estimating F_α and F_β online, the observer compensates for unknown disturbances and parameter mismatch in real time.

$$\begin{cases} \hat{i}_\alpha(k+1) = \hat{i}_\alpha(k) + T_s\hat{F}_\alpha(k) + T_s a_\alpha u_\alpha(k) + T_s U_{\alpha smo} \\ \hat{F}_\alpha(k+1) = \hat{F}_\alpha(k) + T_s g_\alpha U_{\alpha smo} \end{cases} \tag{19}$$

$$\begin{cases} \hat{i}_\beta(k+1) = \hat{i}_\beta(k) + T_s\hat{F}_\beta(k) + T_s a_\beta u_\beta(k) + T_s U_{\beta smo} \\ \hat{F}_\beta(k+1) = \hat{F}_\beta(k) + T_s g_\beta U_{\beta smo} \end{cases} \tag{20}$$

E. OVERALL SENSORLESS MPTC SYSTEM BASED ON ULTRA-LOCAL MODEL

Overall Control Structure is depicted in Fig. 10. Based on the fundamental theory, the proposed control scheme adopts the model-predictive-control framework. Full order adaptive observer for estimating rotor speed and rotor flux online. Since the traditional method's stator current prediction model can't handle motor parameter change very well, ultra-local model enters at prediction step. Ultra-local sliding mode observer estimates F_α, F_β unknowns and uses estimation as correction for stator current predication.

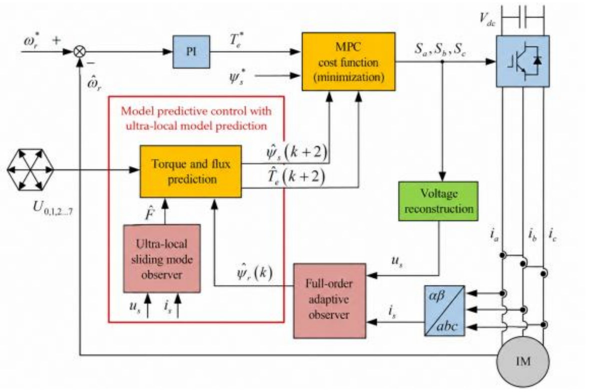

FIGURE 10. Architecture of the ultra-local model-based sensorless predictive control system

Here is how the entire control process can go. First we will sample our stator's currents as well as the recovered voltage of the stator. Following on from this the full order adaptive observer gives us an estimate for the Rotor Speed and Flux. After that, it estimates the unknown disturbance terms in the α-axis and β-axis current model by Ultra Local sliding Mode Observer. After the stator-current estimation is corrected, the corrected values are used to predict the electromagnetic torque and stator flux under each candidate voltage vector. In the last step we choose and apply the voltage vector which leads to least cost function for our inverter.

Compared with the earlier approach of the traditional sensorless MPTC technique, the proposed method does not require such a parameter-dependent model.

In this section we give sensorless Model Predictive Control method for Induction Motors based on Ultra-Local. Original thesis analyzed parameter sensitivities for both traditional predicative controlling algorithms as well as the complete order adaptive observers. It turns out that stator resistance mismatch and mutual inductance mismatch cause errors about how big the magnetic field is and how much it has shifted which then also influences guessing how fast things move around as well as what sort of electrical flow there might be. To increase robustness, we introduce the ultra-local model to reformulate the stator current prediction model. Subsequently, an ultra-local sliding-mode estimator is developed for real-time estimation of the unknown system terms. And so on, the estimate unknown part into predict the part of the sensorless MPTC.

Furthermore, it retains the favorable fast dynamic-response characteristic of MPTC while reducing dependence on accurate motor parameters. In addition, it compensates for speed-estimation errors and external disturbances.

VI. SIMULATION VALIDATION OF THE PROPOSED SENSORLESS PREDICTIVE CONTROL METHOD

A. SIMULATION MODEL

To verify the effectiveness of the proposed method, we built a simulation environment in MATLAB/Simulink based on the induction-motor mathematical model and the predicted-torque control system structure for joint validation. The simulation system mainly consists of the induction motor module, voltage source inverter, full-order adaptive observer, ultra-local sliding mode observer, and predictive torque controller. The overall simulation structure is shown in Fig. 11.

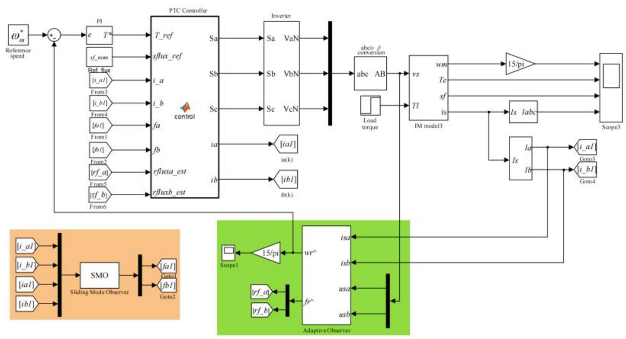

FIGURE 11. Simulation framework of the ultra-local model-based sensorless predictive control system

According to experiment, select the induction motor's simulating parameter. The sampling time is chosen in accordance with the prompt for live operation of our predictive control code. The control system adopts a finite-control-set model predictive torque control method and uses the full-order adaptive observer to estimate the rotor speed and rotor flux linkages online. At the same time, the ultra-local sliding mode observer also estimates unknown disturbances contained in the current prediction model.

Compared with conventional sensorless MPTC, the proposed method incorporates an additional ultra-local model into the stator-current prediction process. Consequently, it is much less susceptible to parameter mismatch and observer estimation errors than the conventional scheme.

B. SIMULATION RESULTS AND ANALYSIS

1) VERIFICATION OF SYSTEM CORRECTNESS

Verifying the rightness of our invented sensorless model predictive control method with ultra-local models was achieved using no-load simulators for differing circumstances first off.

To do a full-speed range test of the motor: the rotation per minute was gradually increased from 60 rpm to 900 rpm, 1500 rpm, 1200 rpm, then reduced back down to 300 rpm. Fig. 12 compares the true speed and the estimated one, and also includes the difference. Fig. 13 gives us the torque and stator current waveform as well.

It can be observed that the speed-estimation error reaches its maximum value during the transition from acceleration to deceleration. After the motor reaches the steady-state condition, the speed-estimation error approaches zero. This

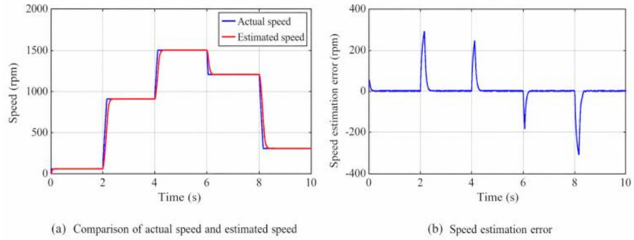

FIGURE 12. Simulation Waveform in Full Speed Range of No-load Operation

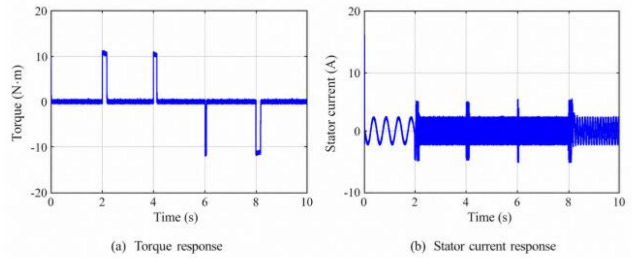

FIGURE 13. Simulation Waveform of Torque and Stator Current in Full Speed Range of No-load Operation

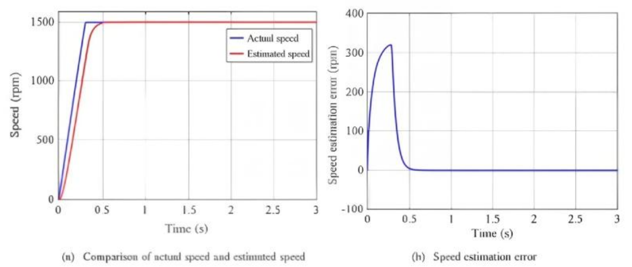

FIGURE 14. Simulation Waveform in Rated Speed of No-load Operation

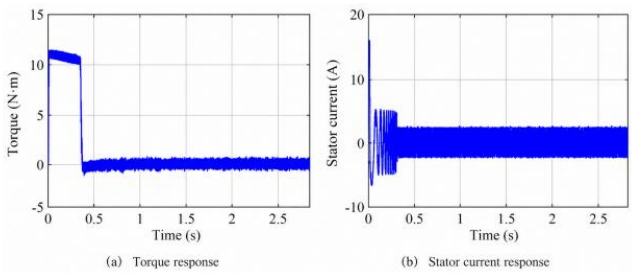

FIGURE 15. No Load Operation Rated Speed Internal Torque and Stator Current Simulation Waveform

demonstrates that favorable speed-estimation performance can be obtained over the whole operating range. During transients, the electromagnetic torque can reach 7.5 N·m under nominal conditions. Rated-Speed Operation: The motor runs at 1500 rpm under no-load conditions. Fig. 14 illustrates the actual speed, estimated speed and speed-estimation error, and Fig. 15 gives the torque and stator-current waveforms.

The results show that the speed estimation error is almost zero in steady state. The torque reaches the limit value during startup and then fluctuates around zero after stabilization. For low-speed operation, the motor was operated at 30 rpm. Fig. 16. shows the speed estimation performance, and Fig. 17. shows the torque and stator current waveforms.

Although the speed error is relatively large during startup, it converges to nearly zero after the system becomes stable.

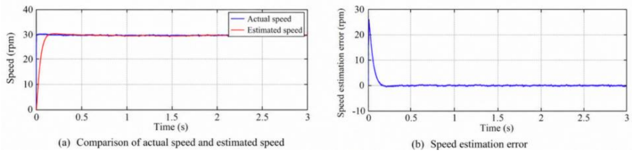

FIGURE 16. Simulation Waveform at Low Speed in No-load Operation

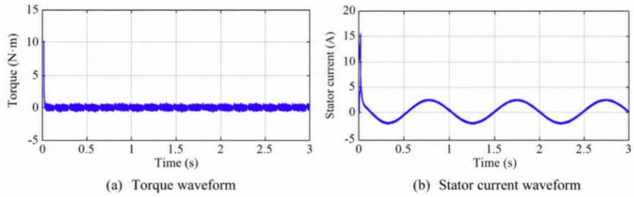

FIGURE 17. Simulation Waveform of Low Speed Internal Torque and Stator Current in No-load Operation

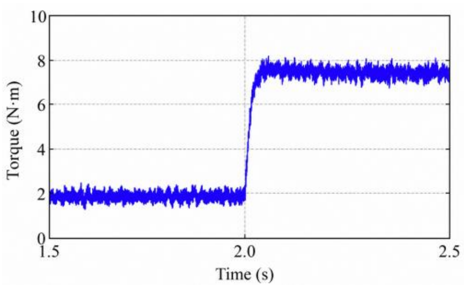

FIGURE 18. The Waveform of Light to Heavy Load Torque

The torque remains close to zero in steady state, and the stator current waveform remains stable, showing that the proposed method also performs well at low speed. To verify the torque response performance, the torque reference was changed from 2 N·m to 7.45 N·m at $t = 2$ s under rated-speed operation. The result is shown in Fig. 18. The torque response time is about 0.04 s, which confirms the fast torque response of finite-control-set model predictive control.

2) SIMULATION RESULTS UNDER SUDDEN LOADING AND UNLOADING

Load disturbance rejection is evaluated with respect to motor which was already running at its rated speed. Load was suddenly put on at $t = 1$ s. Remove the load at $t = 2$ s. Fig. 19 shows the estimated speed and speed estimation error of ultra-local model, while Fig. 20 shows the corresponding result of the traditional one. Under the ultra-local model, the speed drop during loading is about 19 rpm, the speed rise during unloading is about 20 rpm, and the speed estimation error is within approximately ± 11 rpm. Under the traditional model, the speed drop and rise increase to about 30 rpm and 31 rpm, respectively, and the speed estimation error reaches approximately ± 15 rpm. Therefore, the ultra-local model improves load disturbance rejection and speed estimation accuracy.

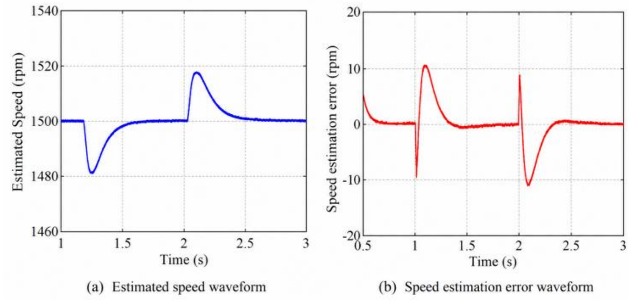

FIGURE 19. Dynamic response under load application and removal at rated speed using the ultra-local model

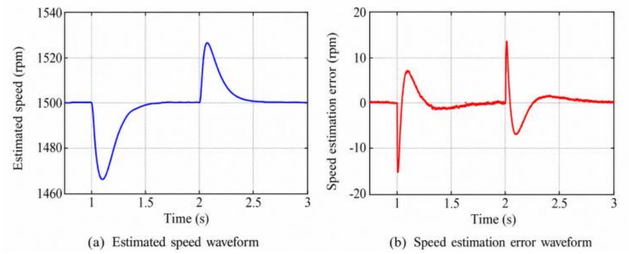

FIGURE 20. Dynamic response under load application and removal at rated speed using the conventional model

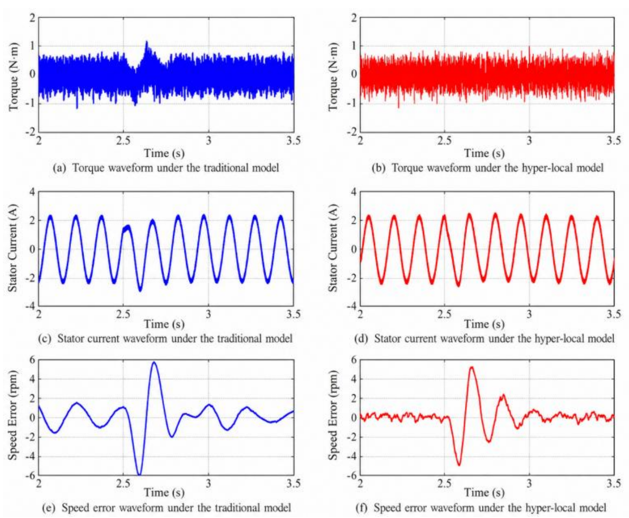

FIGURE 21. Simulation Waveform Comparison (200 rpm)

3) SIMULATION RESULTS UNDER PARAMETER MISMATCH

The proposed technique is made stronger by being tested for parameter mismatches at 200 rpm as well. The stator resistance mismatch leads to a deviation change when $t = 2.5$s where it is $\Delta R_s = 50\%$. Figure 21 shows the comparative traditional models and the ultra-local models. This includes Torque Waveform, Stator Current, Speed Error Waveform. Compared to the traditional model, the ultra-local model reduces torque spike, improves sinusoidal property of stator current, and slightly decreases the speed estimation error after adjustment. This proves that our proposed method can withstand stator resistance mismatch.

For mutual inductance mismatch, the deviation changes to $\Delta L_m = 100\%$ at $t = 2.5$ s. Fig. 22 compares the traditional model and the ultra-local model under the

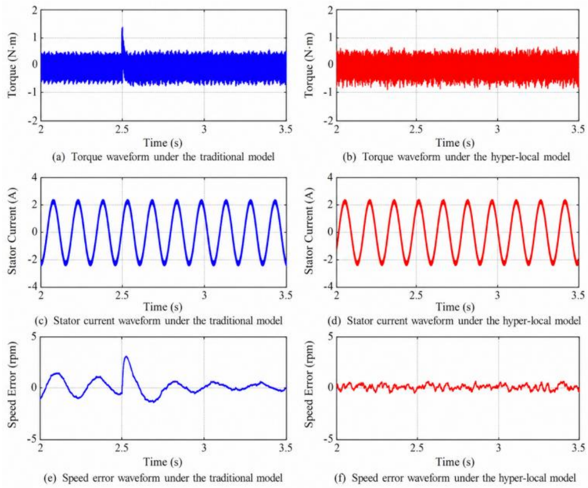

FIGURE 22. Simulation Waveform Comparison (200 rpm) when Mutual Inductance Mismatched

same operating speed. This section verifies the proposed sensorless predictive control strategy through simulation. Compared with the traditional sensorless model predictive control method, the ultra-local model-based strategy shows better load disturbance rejection and stronger robustness when motor parameters vary.

VII. CONCLUSION

The paper first talked about the different mathematical representations for an induction motor using varying reference frames and developed a MPTC system. Traditional speed sensors increased system costs and decreased reliability which makes sensorless Predictive Control interesting. But speed estimation errors and wrong parameters will also reduce its precision, leading to a bad effect on this system. Thus an ultralocal model is used for better robustness in the sensorless predictive control system. Main works of this thesis are:

First, the main control methods for induction motors are reviewed, and the research progress of model predictive control is summarized. The mathematical model of the induction motor and the implementation procedure are explained in detail.

Second, this paper designs and analyzes a full-order adaptive observer for induction motors. The stability and speed-estimation accuracy of the observer are verified by pole-placement and Lyapunov stability theory. Moreover, to enhance robustness, an ultra-local model is introduced to improve the conventional scheme. An ultra-local sliding-mode observer is utilized to estimate unknown disturbances, and the corresponding stability analysis is carried out.

Finally, simulation studies are conducted to evaluate the effectiveness of the proposed method. The results show that the full-order adaptive observer can accurately estimate rotor flux linkage and stator current information, enabling reliable rotor speed estimation without a mechanical speed sensor. Furthermore, the ultra-local model-based predictive control strategy exhibits strong robustness against load disturbances and parameter mismatches, while preserving favorable transient response characteristics and stable operating behavior. The obtained results further confirm the feasibility and robustness of the developed sensorless predictive control strategy for induction motor drive applications.

ACKNOWLEDGMENTS

This work was supported by the National Nature Science Foundation of China (No. 52305048 and No. 52477035), the Zhiyuan Science Foundation of BIPT (No. 2025208 and No. 2024101).

REFERENCES

[1] B. S. Chen and M. X. Chen, *AC Speed Regulation System*. Beijing: China Machine Press, 2005.
[2] F. G. Zhang, G. H. Du, T. Y. Wang, and G. W. Liu, "Review of High-speed Motor Development and Design," *Transactions of China Electrotechnical Society*, vol. 31, no. 7, pp. 1–18, 2016.
[3] C. L. Xia, *Brushless DC Motor Control System*. Beijing: Science Press, 2009.
[4] S. S. Sun and H. Ai, "DSP-based Fuzzy PI Brushless DC Motor Control System," *Small & Special Electrical Machines*, vol. 41, no. 6, pp. 68–71, 2013.
[5] H. L. Zhang, "Research on Brushless DC Motor Controller and Control Algorithm," dissertation, Hangzhou Dianzi University, 2012.
[6] B. S. Chen, *Automatic Control System of Electric Drive*, 3rd ed. Beijing: China Machine Press, 2003.
[7] B. S. Chen and G. Yang, "Three Approaches of High-performance Sensorless AC Drive Control and Development Suggestions," *Electric Drive*, vol. 31, no. 1, pp. 3–8, 2006.
[8] C. Y. Wang, J. K. Xia, and Y. B. Sun, *Modern Motor Control Technology*. Beijing: China Machine Press, 2008.
[9] J. Y. Wang, S. L. An, J. Li, and Y. R. Zhong, "Induction Motor Model Considering Main Magnetic Saturation and Iron Loss," *Transactions of China Electrotechnical Society*, vol. 25, no. 10, pp. 44–50, 2010.
[10] C. J. Li, "Discussion on Variable Frequency Speed Regulation Control System of AC Motor," *Power Electronics*, 2004.
[11] W. Chen, X. H. Jin, L. Cai, and D. G. Xu, "Simulation Study on Light-load Stability of V/F Controlled Induction Motor System," *Proceedings of the CSEE*, vol. 33, no. S1, pp. 211–218, 2013.
[12] W. Chen, R. F. Yang, Y. Yu, G. L. Wang, and D. G. Xu, "A Novel Stability Improvement Method for V/F Controlled Induction Motor Drive Systems," in *2008 International Conference on Electrical Machines and Systems*, 2008, pp. 1073–1076.
[13] K. Lee, W. Yao, B. Chen, Z. Lu, A. Yu, and D. Li, "Stability Analysis and Mitigation of Oscillation in an Induction Machine," *IEEE Transactions on Industry Applications*, vol. 50, no. 6, pp. 3767–3776, 2014.
[14] R. Bharti, M. Kumar, and B. M. Prasad, "V/F Control of Three Phase Induction Motor," in *2019 International Conference on Vision Towards Emerging Trends in Communication and Networking*, 2019, pp. 1–4.
[15] X. T. Garcia, A. Arias, M. G. Jayne, and P. A. Witting, "Direct Torque Control of Induction Motors Utilizing Three-level Voltage Source Inverters," *IEEE Transactions on Industrial Electronics*, vol. 55, no. 5, pp. 956–958, 2008.
[16] H. G. Wang, W. L. Xu, J. Li, and G. Yang, "A Novel Direct Torque Control Strategy for Induction Motors," *Proceedings of the CSEE*, no. 01, pp. 107–111, 2004.
[17] I. M. Alsofyani, K. Y. Kim, S. S. Lee, et al., "A Modified Flux Regulation Method to Minimize Switching Frequency and Improve DTC-hysteresis-based Induction Machines in Low-speed Regions," *IEEE Journal of Emerging and Selected Topics in Power Electronics*, pp. 1–1, 2019.
[18] J. X. Wang and J. G. Jiang, "Variable Structure Direct Torque Control of Matrix Converter-fed Induction Motor Based on Field Orientation," *Proceedings of the CSEE*, vol. 30, no. 06, pp. 57–62, 2010.
[19] F. Blaschke, "The Principle of Field Orientation as Applied to the New Transvector Closed Loop Control System for Rotating Field Motors," *Siemens Review*, vol. 34, no. 11, pp. 217–220, 1972.
[20] A. B. Luis, L. C. Jesus, and L. C. Eduardo, "Speed and Position Controllers Using Indirect Field-oriented Control: A Classical Control Approach," *IEEE Transactions on Industrial Electronics*, vol. 61, no. 4, pp. 1928–1943, 2014.